Structure and properties of layered-perovskite $LaBa_{1-x}Co_2O_{5+\delta}$ ($x = 0-0.15$) as intermediate-temperature cathode material

S.L. Pang [a,b], X.N. Jiang [a,*], X.N. Li [a], H.X. Xu [a], L. Jiang [c], Q.L. Xu [a], Y.C. Shi [a], Q.Y. Zhang [a]

[a] Key Laboratory of Materials Modification by Laser, Ion and Electron Beams, Ministry of Education, Dalian University of Technology, No. 2 Linggong Road, Ganjingzi District, Dalian 116024, China
[b] Institute for Advanced Materials, School of Materials Science and Engineering, Jiangsu University, Zhenjiang, Jiangsu 212013, China
[c] Dalian Institute of Chemical and Physics, CAS, Dalian 116023, China

HIGHLIGHTS

- $LB_{1-x}CO$ ($x = 0-0.15$) oxides have tetragonal layered-perovskite structures at 850 °C−1050 °C.
- $LB_{1-x}CO$ oxides show decreased conductivities with higher Ba-deficiency content.
- Introduction of Ba deficiency results in remarkably decreased ASRs for $LB_{1-x}CO$.
- $LB_{1-x}CO$ ($x = 0.10-0.15$) oxides are promising cathode materials for IT-SOFCs.

ARTICLE INFO

ABSTRACT

Phase structure, structure stability, electrical properties and catalytic activity for oxygen reduction reaction of the Ba-deficient layered-perovskite oxides $LaBa_{1-x}Co_2O_{5+\delta}$ ($LB_{1-x}CO$, $x = 0.00-0.15$) have been studied to determine their viability as cathode material of intermediate-temperature solid oxide fuel cells (IT-SOFCs). $LB_{1-x}CO$ had tetragonal layered-perovskite structure when calcined at 850 °C−1050 °C in air but transformed into cubic structure at higher temperatures. The $LB_{1-x}CO$ oxide exhibited lower electrical conductivities and decreased area-specific resistances (ASRs) on the $Ce_{0.9}Gd_{0.1}O_{1.95}$ (GDC) electrolyte with higher Ba-deficiency content. Among the samples, the $LB_{0.90}CO$ ($x = 0.10$) oxide exhibited the best electrochemical performance with ASR values of 0.118 Ω cm^2 at 600 °C and 0.023 Ω cm^2 at 700 °C respectively, ∼40% lower than the results of the parent oxide ($x = 0$), demonstrating its promising application as cathode materials of IT-SOFCs.

1. Introduction

Solid oxide fuel cells (SOFCs) are chemical−electrical energy conversion devices with the advantages of high working efficiency, low emissions and excellent fuel flexibility. The present research focus in the SOFC field is lowering the cell working temperature to the intermediate-temperature (IT) range of 600 °C−800 °C, in order to extend the choice of component materials, lengthen the cell duration time and realize cost reduction [1,2]. At the lowered temperatures, polarization resistance of the cathode becomes the key factor in determining the overall performance of the IT-SOFCs due to high activation energy for oxygen reduction reaction (ORR) occurring over the cathode [2,3]. Thus, various cathode materials

with high catalytic activity for ORR in the intermediate-temperature range are being pursued [4−9], among which, a series of mixed ionic−electronic conducting (MIEC) $LnBaCo_2O_{5+\delta}$ (LnBCO, Ln = Lanthanide) oxides with double-layered perovskite structures have received much attention due to their greatly enhanced oxygen transport kinetics and widely adjustable oxygen contents in recent years [6−9]. Systematic studies of LnBCO oxides with Ln = Nd^{3+}, Sm^{3+}, Gd^{3+} and Y^{3+} [3], and Pr^{3+}, Nd^{3+}, Sm^{3+} and Gd^{3+} [10,11] have demonstrated that the LnBCO oxides with larger Ln^{3+} ions exhibit better cathode performance due to improved oxygen-ion diffusion and oxygen ionic conductivity. However, the layered-perovskite oxide $LaBaCo_2O_{5+\delta}$ with the largest ion (La^{3+}) among the lanthanide at A-sites was reported to be difficult in synthesis [12] and thus has been less studied. We previously found [13,14] that the $LaBaCo_2O_{5+\delta}$ thin film had extraordinary sensitivity to reducing-oxidizing environment and exceedingly fast surface exchange rate. Very recently, we have synthesized a pure phase of

* Corresponding author. Tel.: +86 41184708380x8204; fax: +86 41184708389.
E-mail address: xnjiang@dlut.edu.cn (X.N. Jiang).

layered-perovskite $LaBaCo_2O_{5+\delta}$ oxide and studied its structural stability and electrical properties with a comparison between the A-site cation-disordered counterpart $La_{0.5}Ba_{0.5}CoO_{3-\delta}$ [15]. LaBaCo$_2$O$_{5+\delta}$ has also been characterized as a cathode material of IT-SOFCs [16], and the results have demonstrated that $LaBaCo_2O_{5+\delta}$ has very good electrochemical performance at temperatures of 700 °C and above, but its resistances at temperatures below 700 °C are still too high for usage (>0.15 Ω cm^2) [17]. Therefore, electrochemical performance of the $LaBaCo_2O_{5+\delta}$ oxide needs further improvement when low working temperatures are desired.

Composite cathode is a commonly used method of improving electrochemical performance of the perovskite-typed oxides [7,18,19]. Jacobson group [7] reported a lower polarization resistance, 0.15 Ω cm^2 at 600 °C for the $PrBaCo_2O_{5+\delta}$–$Ce_{0.9}Gd_{0.1}O_{1.95}$ (1:1 weight ratio) composite cathode than the value of 0.213 Ω cm^2 for the single-phase $PrBaCo_2O_{5+\delta}$ cathode [12]. Introduction of A-site cationic deficiency is another feasible way of improving electrochemical performance of perovskite oxides. Liu et al. [20] obtained an extremely low polarization resistance, 0.046 Ω cm^2, and a very high power density of 1062 mW cm^{-2} at 600 °C for the cation-deficient $Ba_{0.9}Co_{0.7}Fe_{0.2}Nb_{0.1}O_{3-\delta}$ oxide, which was ascribed to generation of more oxygen vacancies. Very recently, we have demonstrated [21,22] that introduction of A-site Ba^{2+} deficiency to layered-perovskite oxide $PrBaCo_2O_{5+\delta}$ significantly improved its electrochemical performance. About 50% decrease in polarization resistances was achieved at temperatures of 600 °C–700 °C for the $PrBa_{0.92}Co_2O_{5+\delta}$ oxide with 8% Ba-deficiency, as compared with the results of the stoichiometric $PrBaCo_2O_{5+\delta}$ cathode fabricated under the same conditions. We conclude that introduction of Ba^{2+} deficiency is an effective way of improving electrochemical performance of the series of $LnBaCo_2O_{5+\delta}$ layered-perovskite oxides. However, since structures, chemical defects and properties of perovskite oxides are basically determined by types and content of its A-site and/or B-site cations [2,3,8,10], the $LnBaCo_2O_{5+\delta}$ oxides with different Ln^{3+} ions at A-sites could probably show different response to introduction of Ba-deficiency. To confirm our assumption, we have studied another Ba-deficient layered-perovskite oxide $LaBa_{1-x}Co_2O_{5+\delta}$ ($LB_{1-x}CO$, $x = 0.00-0.15$) with respect to its phase structure, structural stability, and electrical and electrochemical properties. As expected, electrochemical catalytic activity of the $LB_{1-x}CO$ oxides are greatly enhanced by introduction of Ba^{2+} deficiency, and the results of $LB_{1-x}CO$ are different, in some ways, from the results of the Ba-deficient $PrBa_{1-x}Co_2O_{5+\delta}$ oxides [21,22].

2. Experimental

Layered-perovskite oxides $LaBa_{1-x}Co_2O_{5+\delta}$ ($LB_{1-x}CO$) with A-site Ba-deficiency content $x = 0.00-0.15$ were synthesized via a combined EDTA–citrate complexing sol–gel process, as described in our previous work [16]. Briefly, stoichiometric amounts of nitrates $La(NO_3)_3\cdot6H_2O$ (AR), $Ba(NO_3)_2$ (AR) and $Co(NO_3)_3\cdot6H_2O$ (AR) were firstly dissolved into $EDTA-NH_3\cdot H_2O$ solution (pH ≈ 6) to form an aqueous solution, and then acid$-NH_3\cdot H_2O$ solution (pH ≈ 6) was added at a mole ratio of 1:1:2 for EDTA:total metal ions:citric acid. The mixed solution was heated at 80 °C and 150 °C subsequently for several hours to obtain a dark dry foam structure. After decomposed on a hot plate, the $LB_{1-x}CO$ powders were calcined at 600 °C (12 h, in air), 900 °C (12 h, in air), and 1200 °C (7 h, in Ar) in sequence, forming a pure phase of A-site cation-ordered perovskite structure. Since the cathode of SOFC works in air atmosphere, the as-synthesized powders were then fired in air at the temperature of 850 °C–1150 °C for 4 h to study their phase stabilities.

Phase structures of the $LB_{1-x}CO$ ($x = 0.00-0.15$) powders calcined at various temperatures were characterized by X-ray

diffraction measurement (XRD, Rigaku D/Max 2400). The XRD patterns were collected at room temperature with step size of 0.02° in 2θ over the scanning angular range of 20−80°. Electrical conductivities of the oxides were measured in air in the temperature range of 150 °C−850 °C with an interval of 50 °C by a DC four-electrode method. Electrochemical performance of the porous $LB_{1-x}CO$ ($x = 0.00-0.15$) cathodes were characterized by electrochemical impedance spectra (EIS) measurements using $Ce_{0.9}Gd_{0.1}O_{1.95}$ (GDC) as electrolyte in a $LB_{1-x}CO/GDC/LB_{1-x}CO$ symmetrical cell configuration. Dense solid GDC pellets with diameters of ∼10 mm and thickness of ∼1 mm were obtained by uniaxially pressing GDC powders into disk-shape pellets and then sintered at 1350 °C for 7 h in air. For fabrication of porous cathode layers, the $LB_{1-x}CO$ inks prepared by mixing the cathode powders with α-terpineol and ethyl cellulose were screen-printed onto both sides of the polished GDC pellets and followed by sintering at 1000 °C for 2 h in air. The EIS data were collected by a Solartron 1260 Frequency Response Analyzer combined with a Solartron 1287 potentiostat under open circuit voltage (OCV) condition as a function of temperature (600 °C−800 °C) in flowing air. Microstructures of the post-test cells were observed with a scanning electron microscopy (SEM, Hitachi S-4800).

3. Results and discussion
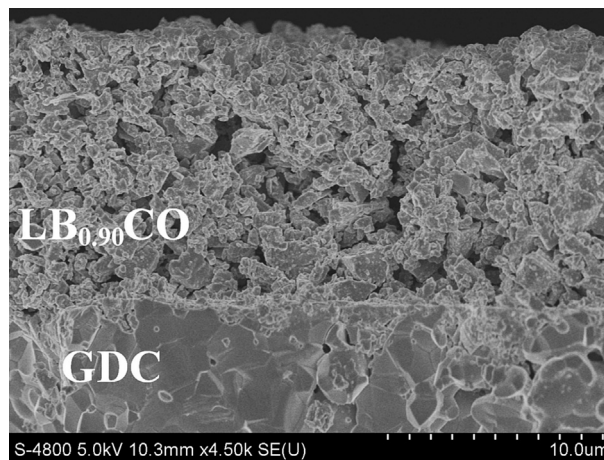
3.1. Phase structure and cathode microstructure

As is known [23,24], phase structure of the (La,Ba,Co)O compound changes with synthesis and post-annealing conditions such as temperature and atmosphere. In our previous work [15,16], we obtained both A-site La^{3+}/Ba^{2+} cation-ordered and disordered (La,Ba,Co)O perovskite oxides and found that these two structures exhibited different electrical and electrochemical properties. The cation-ordered sample was observed to transform into cation-disordered phase when annealed at temperatures above 1050 °C in air [16]. In this work, we introduced Ba-deficiency into the cation-ordered $LaBaCo_2O_{5+\delta}$ (LBCO) oxide. In order to check possible influence of the Ba-deficiency upon stability of the phase structure, the as-synthesized $LB_{1-x}CO$ ($x = 0.00-0.10$) powders were fired at various temperatures in air and were characterized by XRD measurement. As a typical example, the XRD patterns of $LB_{0.90}CO$ oxide with Ba-deficiency content $x = 0.10$ calcined at temperatures of 850 °C−1150 °C were shown in Fig. 1a. The XRD patterns for the samples calcined at 1100 °C−1150 °C were indexed with a cubic Pm-3m structure with $a_p = 3.899$ Å, which indicates that the La^{3+} and Ba^{2+} cations are randomly distributed at A-sites of the perovskite structure [15,23,24]. In contrast, the samples calcined at 850 °C−1050 °C were indexed with a tetragonal P4/mmm space group with lattice parameters of $a = b = 3.919$ Å $\approx a_p$ and $c = 7.730$ Å $\approx 2a_p$. The doubled c-axis ($c \approx 2a_p$) demonstrates that a layered-perovskite structure with LaO_δ/BaO layers alternating stacking along the c-axis characteristic of the A-site La^{3+}/Ba^{2+} cationic ordering was formed [23,24]. Thus, a phase transition with calcination temperatures has occurred in the Ba-deficient $LB_{0.90}CO$ oxide similar to the parent LBCO ($x = 0$) oxide [16], which was probably associated with the promoted cationic interdiffusion at high temperatures. Moreover, since the XRD patterns were collected at room temperature, these results have further indicated that the A-site La^{3+}/Ba^{2+} cationic disordering in $LB_{0.90}CO$ formed at the high temperatures can be well kept during the cooling process of the sample. Rautama et al. [23] and Nakajima et al. [24] also reported that similar results for the LBCO oxides without Ba-deficiencies. Fig. 1b shows the XRD patterns of the $LB_{1-x}CO$ ($x = 0.00-0.15$) powders calcined at 1000 °C for 4 h in air. All the XRD patterns were indexed with a tetragonal P4/mmm structure, and no impurity phases were found. This
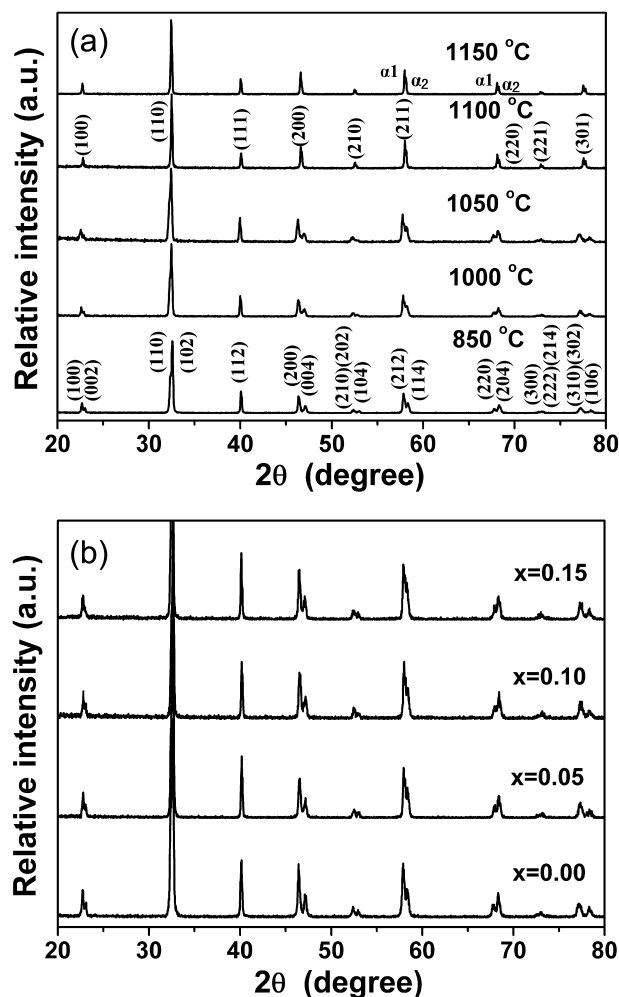
Fig. 1. (a) XRD patterns of LB$_{0.90}$CO ($x = 0.10$) oxide calcined at various temperatures in air and (b) XRD patterns of the LB$_{1-x}$CO ($x = 0.00$–0.15) oxides calcined at 1000 °C for 4 h in air. The splitting diffraction peaks, marked with "α1" and "α2", at the high 2θ angles of the XRD patterns for 1100 °C and 1150 °C in (a) come from diffractions from respective Kα1 and Kα2 X-rays.

Fig. 2. Typical cross-sectional SEM image of the LB$_{1-x}$CO/GDC interface fired at 1000 °C in air.

structure with uniformly distributed micrometer-sized pores, which is advantageous for gas-diffusion through the cathode. Clear and good binding between the porous cathode layer and the dense GDC electrolyte layer was obtained, which ensures the low cathode/electrolyte interface-resistances in the LB$_{1-x}$CO/GDC/LB$_{1-x}$CO symmetrical cell. The other LB$_{1-x}$CO/GDC interfaces have the similar microstructures.

3.2. Electrical conductivity

Fig. 3 presents electrical conductivities of the LB$_{1-x}$CO ($x = 0.00$–0.15) oxides measured at various temperatures in air. The values of conductivity in the measured temperature range (150 °C–850 °C) are above 280 S cm^{-1} for all the samples, meeting the requirement of electrical conductivity (>100 S cm^{-1}) for use as IT-SOFC cathodes [27]. Cobalt-based perovskite oxides are mixed ionic and electronic conductors (MIEC) due to co-presence of electron holes ($h^{\bullet}$) and oxygen vacancies ($V_O^{\bullet\bullet}$) [2,12]. Because the oxygen ionic conductivity is much lower than the electronic conductivity in the MIEC systems, the conductivity shown in Fig. 3 was assumed to be primarily electronic conductivity. All the LB$_{1-x}$CO samples experience a decrease in conductivity with increasing temperatures, which is related to reduction of Co^{4+} to Co^{3+} ions caused by

indicates that the A-site Ba-deficiency content (x) in the LB$_{1-x}$CO oxide can reach a high level of 15% under the present conditions. In addition, no obvious position shifts of the diffraction peaks were observed for the LB$_{1-x}$CO oxides with different Ba-deficiency contents, suggesting that introduction of the Ba-deficiency at contents up to $x = 0.15$ hardly changed the lattice parameters of LB$_{1-x}$CO. In contrast, the Ba-deficiency content in PrBa$_{1-x}$Co$_2$O$_{5+\delta}$ oxide was only limited to 8% and structural shrinkage was observed with higher Ba-deficiency contents [22]. These structural differences might be associated with different sizes of the A-site cations (La^{3+} and Pr^{3+}) in these two layered-perovskite oxides.

To avoid phase transition of the LB$_{1-x}$CO oxides, we chose 1000 °C as the firing temperature for fabrication of the LB$_{1-x}$CO cathode layer in the LB$_{1-x}$CO/GDC/LB$_{1-x}$CO symmetrical cells. In our recent work [16], we have found that the LBCO cathode is chemically stable with GDC electrolyte at the firing temperature of 1000 °C. Some researchers [25,26] also reported that the cathodes fired at 1000 °C exhibited the better electrochemical performance than the cathodes fabricated at other temperatures. Fig. 2 is the typical microstructure of the as-prepared LB$_{1-x}$CO/GDC interface after the impedance measurement. It is observed that the cathode with an average thickness of ∼13 μm possesses a homogeneous
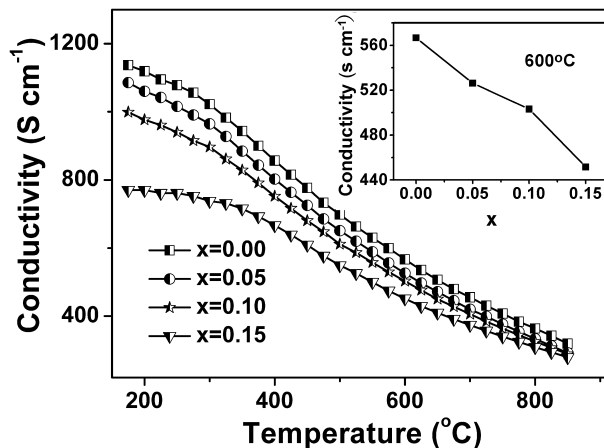

Fig. 3. Temperature-dependence of electrical conductivities of the LB$_{1-x}$CO ($x = 0.00$–0.15) oxides with an inset of electrical conductivity at 600 °C as a function of Ba-deficiency content (x).

thermal-driven releasing of lattice oxygen [3,12]. Furthermore, across all the x values examined, the electrical conductivities of $LB_{1-x}CO$ decreased with higher Ba-deficiency content from $x = 0.00$ to $x = 0.15$, as shown in the inset. This suggests that the charge compensation mechanism in the $LB_{1-x}CO$ oxides is not oxidation of B-site Co^{3+} to Co^{4+} ($h^{\cdot}$, the electronic charge carriers in the p-type semiconductors), but rather the formation of oxygen vacancies, similar with the cases in cation-deficient perovskite oxides of $(Ba_{0.5}Sr_{0.5})_{1-x}Co_{0.8}Fe_{0.2}O_{3-\delta}$ ($x = 0–0.15$) [28] and $La_{0.6}Sr_{0.4-x}Co_{0.2}Fe_{0.8}O_{3-\delta}$ ($x = 0–0.2$) [29]. Thus, with higher Ba^{2+} deficiency, more oxygen vacancies could be generated in the $LB_{1-x}CO$ oxides. On the contrary, Yang et al. [30] found a gradual increase in conductivity with increasing Ba^{2+} deficiency in $Ba_{1-x}Co_{0.7}Fe_{0.2}Nb_{0.1}O_{3-\delta}$ ($x = 0.00–0.15$) oxides, and we observed a conductivity down–up transition with higher Ba^{2+} deficiency in $PrBa_{1-x}Co_2O_{5+\delta}$ oxide ($x = 0.00–0.08$) [22]. Such different electrical conduction behaviors in these cation-deficient perovskite oxides suggest different charge compensation mechanisms, by formation of oxygen vacancies and/or oxidation of B-site ions to a higher valence, for compensation of negative charges induced by introduction of the A-site cationic deficiency.

3.3. Electrochemical performance

To study the effect of Ba-deficiency on electrochemical performance of $LB_{1-x}CO$ ($x = 0.00–0.15$) oxides, electrochemical impedance spectra (EIS) measurements were carried out with the $LB_{1-x}CO/GDC/LB_{1-x}CO$ symmetrical cells at various temperatures in air. Fig. 4 shows a typical set of Nyquist plots of the EIS data with frequencies ranging from 0.1 Hz to $\sim 10^4$ Hz. The ohmic resistances arising from the GDC electrolyte and lead wires were normalized to zero for clarity. One large depressed semi-circle was observed at 600 °C, while a small arc appeared at 650 °C and became bigger gradually at higher temperatures up to 800 °C. This suggested that the rate-limiting elementary steps involved in the cathode reaction

changed with the temperature [20,22,26,28]. With the EIS results, the area specific resistances (ASRs) of the $LB_{1-x}CO$ cathodes were calculated using the equation of ASR = $Rp \times A/2$, where A is geometric electrode area and Rp is the electrode polarization resistance, which corresponds to the difference between the intercepts with the real axis at the highest and lowest frequency in the EIS plots [4,18]. The ASR data are shown in Fig. 5. The activation energy (Ea) for each cathode was also calculated from the Arrhenius plot of ASR (Fig. 5a). It is observed that, for each cathode, the ASR value decreases with higher temperatures as expected since the oxygen reduction reaction occurring over the cathode has positive activation energy; and the value of Ea decreases slightly with higher Ba^{2+}-deficiency content with an exception of $x = 0.15$; on the other hand, as clearly shown in Fig. 5b, at the same temperatures, the ASR value of the $LB_{1-x}CO$ cathodes remarkably decreases with higher Ba-deficiency content from $x = 0.00$ to $x = 0.10$, while the data of the sample with $x = 0.15$ are slightly bigger than the sample of $x = 0.10$. Among all the samples, the $LB_{0.90}CO$ ($x = 0.10$) and $LB_{0.85}CO$ ($x = 0.15$) oxides exhibited much better electrochemical performance than the $LB_{1-x}CO$ oxides with lower Ba-deficiency content ($x = 0$ and 0.05). The ASR values range from 0.118 Ω cm^2 at 600 °C to 0.007 Ω cm^2 at 800 °C for $LB_{0.90}CO$ and from 0.130 Ω cm^2 at 600 °C to 0.008 Ω cm^2 at 800 °C for $LB_{0.85}CO$, which are much lower than the criterion of resistance (0.15 Ω cm^2) as a cathode material of SOFCs [17]. In particular, the ASR values of $LB_{0.90}CO$ at 600 °C and 700 °C are only 0.118 Ω cm^2 and 0.023 Ω cm^2 respectively, $\sim 40\%$ lower than the results of the parent LBCO ($x = 0$) oxide (0.195 Ω cm^2 at 600 °C and 0.039 Ω cm^2 at 700 °C). These ASR values are also much lower than those of the cation-disordered $La_{0.5}Ba_{0.5}CoO_{3-\delta}$ cathode (0.15 Ω cm^2 at 600 °C and 0.041 Ω cm^2 at 700 °C) [19], and are comparable with, if not lower than, the results of $La_{0.6}Sr_{0.4}Co_{0.2}Fe_{0.8}O_{3-\delta}$ (0.23 Ω cm^2 at 650 °C and 0.03 Ω cm^2 at 800 °C) [31], $Ba_{0.5}Sr_{0.5}Co_{0.8}Fe_{0.2}O_{3-\delta}$ (0.172 Ω cm^2 at 600 °C and 0.042 Ω cm^2 at 700 °C) [32], as well as $PrBa_{1-x}Co_2O_{5+\delta}$ with 8% Ba-deficiency at A-sites (0.093 Ω cm^2 at 600 °C and

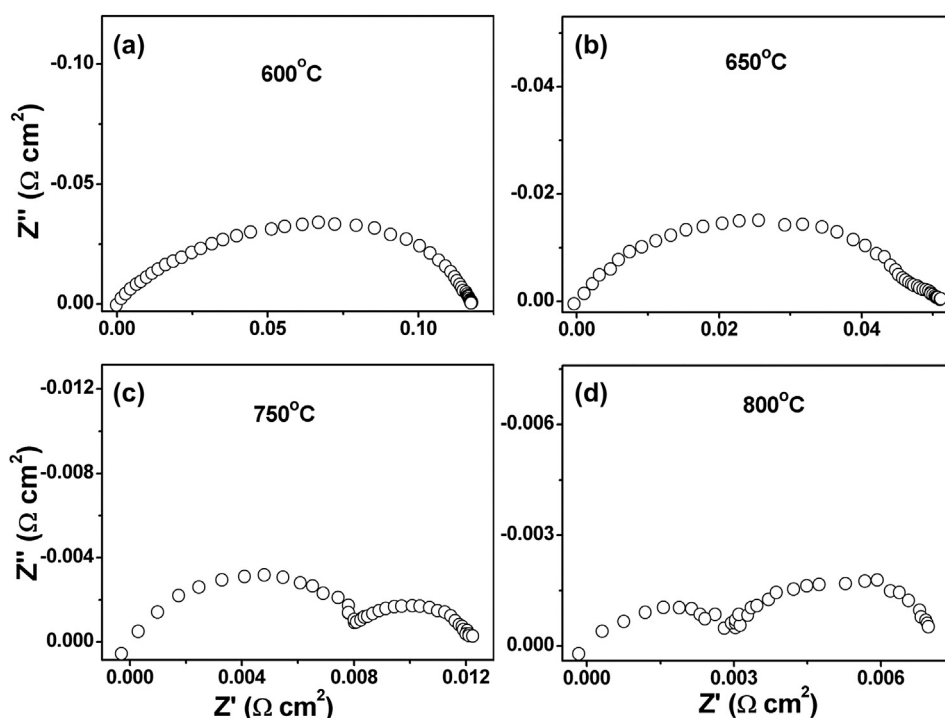**Fig. 4.** EIS results of the $LB_{0.90}CO/GDC/LB_{0.90}CO$ symmetrical cell measured at various temperatures in air. The frequency of the impedance spectra is in the range of $0.1–10^4$ Hz.
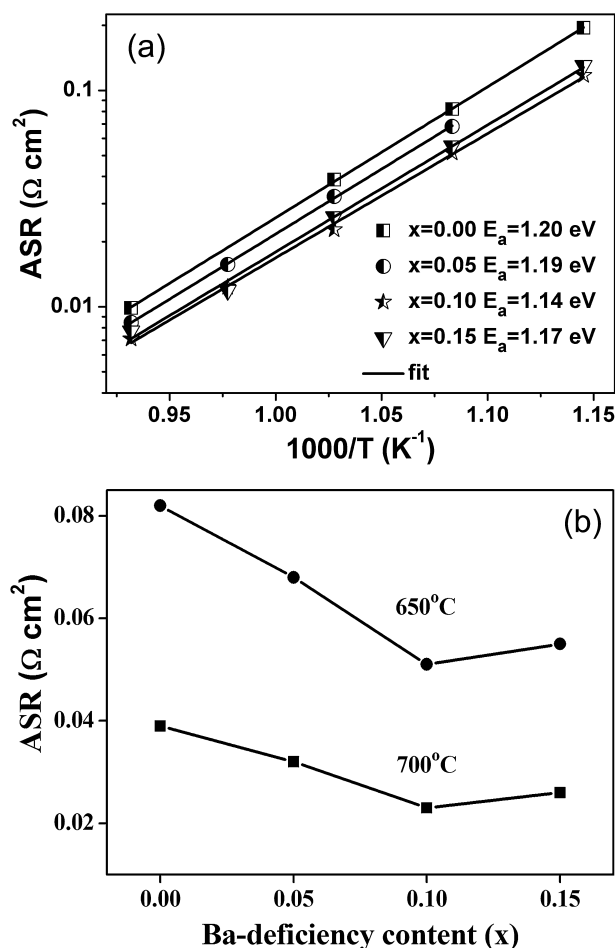
Fig. 5. (a) Arrhenius plots of area-specific resistance (ASR) of $LB_{1-x}CO$ ($x = 0.00-0.15$) cathodes on the GDC electrolyte with the results of activation energies (Ea); (b) ASR values at 650 °C and 700 °C as a function of Ba-deficiency content (x).

0.024 Ω cm^2 at 700 °C) [21]. These results have demonstrated that introduction of Ba^{2+}-deficiency greatly improved electrochemical performance of the $LB_{1-x}CO$ oxides.

Several factors might have contributed to this performance improvement. Firstly, as discussed above based on the electrical conductivities (Fig. 3), more oxygen vacancies could be generated for charge compensation in the $LB_{1-x}CO$ oxides with higher Ba-deficiency content from $x = 0$ to $x = 0.15$. It is well known that increased concentration of oxygen vacancy in the perovskite oxides is advantageous for the oxygen surface exchange and oxygen ionic bulk transport and helps improve the catalytic activities for oxygen reduction reaction, thus resulting in low polarization resistances of the cathodes [2,7,20]. However, recent simulation work by Seymour et al. [33] has suggested that the oxygen vacancies at a high concentration in the series of $LnBaCo_2O_{5.5}$ double-layered perovskite oxides would be trapped by forming clusters with the Ba'_{Ln} antisite defects, which resulted in lowering of the oxygen ionic diffusivity [34]. This factor could be the possible reason for the slightly bigger ASR values of the $LB_{0.85}CO$ ($x = 0.15$) cathode than the $LB_{0.90}CO$ ($x = 0.10$) cathode as shown in Fig. 5, since the $LB_{0.85}CO$ oxide was esteemed from the conductivity results to have relatively more oxygen vacancies; The simulation results [33] have also indicated that these $V_O^{\cdot\cdot}$-associated clusters are more readily formed in the $LaBaCo_2O_{5.5}$ oxide with the largest lanthanide ion La^{3+} at A-sites than the other $LnBaCo_2O_{5.5}$ oxides, such as $PrBaCo_2O_{5.5}$; and this conclusion is consistent with our previous experimental results

[22] that the $PrBa_{1-x}Co_2O_{5+\delta}$ oxide exhibits monotonously decreasing polarization resistance with higher Ba-deficiency content from $x = 0$ to $x = 0.08$ (bigger x caused impurity phases), different from the case of $LaBa_{1-x}Co_2O_{5+\delta}$ studied in this work. However, considering the small difference of ASRs between these two samples ($x = 0.10$ and $x = 0.15$), influence of microstructure of the cathode layer on the electrochemical reactivity could not be completely excluded, although both cathodes layers were prepared under the same conditions. Secondly, distribution of oxygen vacancies and pathway of the oxygen ionic diffusion also influences oxygen transport kinetics and electrochemical performance of the cathodes [6–8]. In our previous work regarding Ba-deficient PBCO [22], we have given a general description of this factor with effect on the electrochemical performance. Here with the sample of Ba-deficient $LB_{1-x}CO$, we address this effect in a more explicit way with structural illustration in Fig. 6. As is shown, in the layered-perovskite LnBCO oxides, oxygen vacancies (V_1) are preferably located in the LnO_δ layer due to the large difference in radius of the Ln^{3+} and Ba^{2+} ions [11,35]. A number of theoretical studies [33,36] have suggested that the oxygen ion transport in the LnBCO oxides is anisotropic with the oxygen ions moving easily in the LnO_δ and CoO_2 layers but not in the BaO layers, as indicated by the solid-line arrows in Fig. 6. A very recent work [35] has experimentally demonstrated this anisotropic oxygen ion diffusion in the layered-perovskite $PrBaCo_2O_{5+\delta}$ by obtaining a larger oxygen diffusion coefficient for the oxygen diffusion on the "*ab*-plain" than that along the "*c*-axis" orientation. This result implies that enhancement of the oxygen ion diffusion along the "*c*-axis" orientation while maintaining the fast diffusion on the "*ab*-plain" could facilitate the oxygen diffusion throughout the whole lattice structure and thus help improve electrochemical performance of the layered-perovskite oxides. As illustrated in Fig. 6, in the layered-perovskite $LB_{1-x}CO$ oxides, deficiency of A-site Ba^{2+} ions (□) is expected to generate oxygen vacancies (V_2), if there are any, preferably on the BaO layers due to break of the Ba–O bonds. Formation of oxygen vacancies on the BaO layers provides the available sites for the oxygen ionic diffusion along the *c*-axis orientation, as indicated by the dash-line arrows in Fig. 6. In this way, the aniso-tropic oxygen ionic diffusion on the "*ab*-plain" via the possible pathways indicated by the solid-line arrows, as reported for the stoichiometric layered-perovskite LnBCO oxides [11], could be extended to three-dimensional (3D) orientations. This 3D oxygen
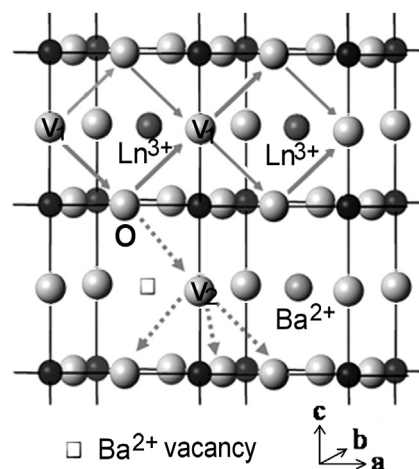

Fig. 6. Illustration of three-dimensional oxygen ionic transport in the Ba-deficient $LnBa_{1-x}Co_2O_{5+\delta}$ (Ln^{3+} = La^{3+}) oxide with a layered-perovskite structure. The solid-line arrows and the dash-line arrows indicate the possible oxygen diffusion path-ways on the "*a–b* planes" and along the *c*-axis orientation, respectively.

ion diffusion with shortened pathways is possibly another contribution to the improved electrochemical performance of the $LB_{1-x}CO$ oxide with higher Ba-deficiency content [11,12], which, however, needs further confirmation by theoretical simulations and/or experimental measurements of oxygen ionic diffusion coefficients.

4. Conclusion

A-site Ba-deficient layered-perovskite oxide $LB_{1-x}CO$ ($x = 0.00–0.15$) experiences a phase transition from tetragonal layered-perovskite structure to cubic perovskite structure at the calcination temperature above 1050 °C. Electrical conductivity of $LB_{1-x}CO$ decreases with higher Ba-deficiency content, suggesting a dominant charge compensation mechanism by formation of oxygen vacancies. Due to increased concentration of oxygen vacancies and realization of three-dimensional oxygen ionic diffusion by introduction of Ba-deficiency, electrochemical performance of the $LB_{1-x}CO$ ($x = 0.10, 0.15$) oxides is greatly improved. Area-specific resistances (ASRs) of the $LB_{1-x}CO$ cathodes on the GDC electrolyte decrease with higher Ba-deficiency content. The $LB_{0.9}CO$ oxide with Ba-deficiency content $x = 0.10$ exhibits the best electrochemical performance among the samples, with ASR values ∼40% lower than the results of the parent LBCO ($x = 0$) oxide. These preliminary results have demonstrated that the Ba-deficient layered-perovskite oxide $LB_{0.90}CO$ is a promising cathode material for IT-SOFCs because of its excellent electrochemical performance.

Acknowledgments

References

[1] B.C.H. Steele, A. Heinzel, Nature 414 (2001) 345–352.
[2] S.B. Adler, Chem. Rev. 104 (2004) 4791–4843.
[3] J.H. Kim, A. Manthiram, J. Electrochem. Soc. 155 (2008) B385–B390.
[4] Q. Su, S. Cho, Z. Bi, A.P. Chen, H.Y. Wang, Electrochim. Acta 56 (2011) 3969–3974.
[5] J.H. Kim, Y.N. Kim, Z.H. Bi, A. Manthiram, M.P. Paranthaman, A. Huq, Electrochim. Acta 56 (2011) 5740–5745.
[6] A.A. Taskin, A.N. Lavrov, Y. Ando, Appl. Phys. Lett. 86 (2005), 091910-1–3.
[7] G. Kim, S. Wang, A.J. Jacobson, L. Reimus, P. Brodersen, C.A. Mims, J. Mater. Chem. 17 (2007) 2500–2505.
[8] A. Tarancón, M. Burriel, J. Santiso, S.J. Skinner, J.A. Kilner, J. Mater. Chem. 20 (2010) 3799–3813.
[9] C. Frontera, A. Caneiro, A.E. Carrillo, J. Oró-Solé, J.L. García-Muñoz, Chem. Mater. 17 (2005) 5439–5445.
[10] Q.J. Zhou, F. Wang, Y. Shen, T.M. He, J. Power Sources 195 (2010) 2174–2181.
[11] J.H. Kim, L. Mogni, F. Prado, A. Caneiro, J.A. Alonso, A. Manthiram, J. Electrochem. Soc. 156 (12) (2009) B1376–B1382.
[12] K. Zhang, L. Ge, R. Ran, Z.P. Shao, S.M. Liu, Acta Mater. 56 (2008) 4876–4889.
[13] J. Liu, M. Liu, G. Collins, C.L. Chen, X.N. Jiang, W.Q. Gong, et al., Chem. Mater. 22 (2010) 799–802.
[14] X.N. Jiang, S. Wang, G. Kim, J. Liu, M. Liu, W.Q. Gong, et al., Solid-State Ionics 2008, Symposium, 2009, pp. P15–P20.
[15] S.L. Pang, X.N. Jiang, X.N. Li, Q. Wang, Q.Y. Zhang, Mater. Chem. Phys. 131 (2012) 642–646.
[16] S.L. Pang, X.N. Jiang, X.N. Li, Z.X. Su, H.X. Xu, Q.L. Xu, C.L. Chen, Int. J. Hydrogen Energy 37 (2012) 6836–6843.
[17] B.C.H. Steele, Solid State Ion. 86–88 (1996) 1223–1234.
[18] H. Gu, H. Chen, L. Gao, L. Guo, Electrochim. Acta 54 (2009) 7094–7098.
[19] S.L. Pang, X.N. Jiang, X.N. Li, Q. Wang, Z.X. Su, Int. J. Hydrogen Energy 37 (2012) 2157–2165.
[20] Z. Liu, L.Z. Cheng, M.F. Han, J. Power Sources 196 (2011) 868–871.
[21] S.L. Pang, X.N. Jiang, X.N. Li, Q. Wang, Z.X. Su, Q.Y. Zhang, Int. J. Hydrogen Energy 37 (2012) 3998–4001.
[22] S.L. Pang, X.N. Jiang, X.N. Li, Q. Wang, Z.X. Su, J. Power Sources 204 (2012) 53–59.
[23] E.L. Rautama, P. Boullay, A.K. Kundu, V. Caignaert, V. Pralong, M. Karppinen, et al., Chem. Mater. 20 (2008) 2742–2750.
[24] T. Nakajima, M. Ichihara, Y. Ueda, J. Phys. Soc. Jpn. 74 (5) (2005) 1572–1577.
[25] S.Q. Lü, Y. Ji, X.W. Meng, G.H. Long, T. Wei, Y.L. Zhang, T.Q. Lü, Electrochem. Solid-State Lett. 12 (6) (2009) B103–B105.
[26] D.J. Chen, R. Ran, Z.P. Shao, J. Power Sources 195 (2010) 4667–4675.
[27] E. Boehm, J.M. Bassat, M.C. Steil, P. Dordor, F. Mauvy, J.C. Grenier, Solid State Sci. 5 (2003) 973–981.
[28] W. Zhou, R. Ran, Z.P. Shao, W.Q. Jin, N.P. Xu, J. Power Sources 182 (2008) 24–31.
[29] G.Ch. Kostogloudis, Ch. Ftikos, Solid State Ion. 126 (1999) 143–151.
[30] Z.B. Yang, M.F. Han, P.Y. Zhu, F. Zhao, F.L. Chen, Int. J. Hydrogen Energy 36 (2011) 9162–9168.
[31] A. Esquirol, N.P. Brandon, J.A. Kilner, M. Mogensenb, J. Electrochem. Soc. 151 (11) (2004) A1847–A1855.
[32] R. Su, Z. Lü, K.F. Chen, N. Ai, S.Y. Li, B. Wei, et al., Electrochem. Commun. 10 (2008) 844–847.
[33] I.D. Seymour, A. Chroneos, J.A. Kilner, R.W. Grimes, Phys. Chem. Chem. Phys. 13 (2011) 15305–15310.
[34] D. Parfitt, A. Chroneos, A. Tarancon, J.A. Kilner, J. Mater. Chem. 21 (7) (2011) 2183–2186.
[35] M. Burriel, J. Pena-Martínez, R.J. Chater, S. Fearn, A.V. Berenov, S.J. Skinner, J.A. Kilner, Chem. Mater. 24 (2012) 613–621.
[36] J. Hermet, G. Geneste, G. Dezanneau, Appl. Phys. Lett. 97 (17) (2010) 174102–174104.